

# ACCURACY ANALYSIS OF EXTENDED FINITE ELEMENT METHOD FOR TENSION OF PLATE WITH A CENTRAL CRACK

J. ŽIVKOVIĆ<sup>1</sup> G. JOVIČIĆ<sup>1</sup> M. ŽIVKOVIĆ<sup>1</sup>  
R. SLAVKOVIĆ<sup>1</sup>

**Abstract:** *The accuracy of the Extended Finite Element Method (XFEM) in solving problems of straining plate with central crack is analyzed. Numerical solutions for displacements and stresses are compared with analytical solutions, while numerical solutions for stress intensity factor are compared with empirical solutions. The impact of the mesh density and near tip (NT) enrichment function are investigated, as well as the impact of the size of the integration domain of J integral used to calculate stress intensity factor  $K_I$ . The use of fine mesh and the NT enrichment functions increase the accuracy of the solution.*

**Key words:** *accuracy analysis, XFEM, mesh density, NT functions, stress intensity factor.*

## 1. Introduction

The extended finite element method, XFEM, reduce computational fracture mechanics problems by not requiring the finite element mesh to coincide with cracks. XFEM is based on using enrichment functions at finite elements that are crossed by the crack. Basis of the XFEM method developed by Belytchko and Black [1], were presented in [4] for the two-dimensional cracks.

Creating a model using XFEM is divided into two steps [3-6]: generation of the mesh for the geometric domain without including cracks, and enriching the finite element approximation by additional functions that model the cracks, without explicitly separating sides of the cracks. There are two enriching functions in

XFEM for fracture mechanics: discontinuity Heaviside step functions (H) and asymptotic near tip functions (NT).

The goal of this paper is to analyze the accuracy of the Extended finite element method for 2D problem, by comparing the obtained numerical results with analytical and empirical solutions.

## 2. Approximation in XFEM

The approximation of displacement in the XFEM is decomposed into a continuous and enrichment part, as

$$u(x) = u_{con}(x) + u_{enrh}(x) \quad (1)$$

where the first addend is standard approximation in the FEM, and second is enrichment part of displacement approximation around the crack. The

---

<sup>1</sup> Faculty of engineering, University of Kragujevac, Serbia.

region of the crack for enrichment by H and NT functions is shown in Figure 1 [5].

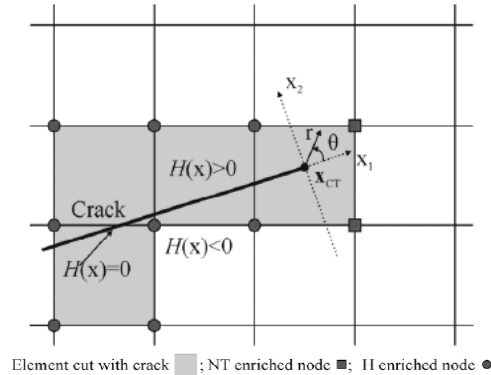
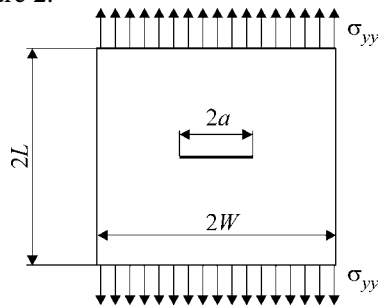


Fig. 1. Enriched region of a crack

### 3. Numerical experiments

Numerical experiments which aimed to demonstrate the impact of mesh parameters and types of nodes enrichment on the accuracy of numerical solutions were performed. Those experiments were performed on a test example of the plate with a central crack, as an example that has strong open discontinuities in fields of displacements. Data for the geometry, material parameters and load are given in Figure 2.



$\sigma_{yy} = 6.89 \text{ KPa}$ ,  $W = 254 \text{ mm}$ ,  $L = 127 \text{ mm}$   
 $a = 127 \text{ mm}$ ,  $E = 2.068 \times 10^5 \text{ MPa}$ ,  $\nu = 0.3$   
 $t = 25.4 \text{ mm}$

Fig. 2. Plate with a central crack

Using the symmetry conditions, only the

right half of the plate was modeled using the XFEM method [4]. The following effects were investigated: 1) density of the mesh, 2) enrichments with NT functions around crack tip, 3) the size of the integration domain of J integral, used to calculate stress intensity factor  $K_I$ . The plate was modeled with 10x10, 20x20, 40x40 and 80x80 elements. The influence of enrichment functions around crack tip was analyzed in two ways: 1) nodes of elements that are crossed by the crack are enriched with Heaviside function and nodes around the crack tip are enriched with NT (H+NT), 2) nodes of elements that are crossed by the crack are enriched only with Heaviside function (H).

In examining the impact of integration domain of J integral, the following relations between radius and crack length were used  $r/a$  (%): 10, 15, 20, 25, 30, 35, 40 и 45%. One integration domain is given in Figure 3, [4].

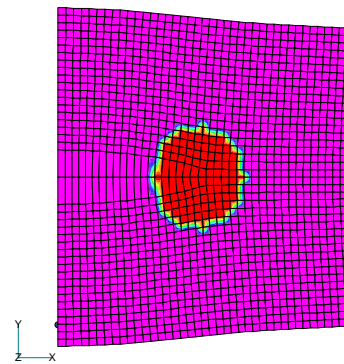


Fig. 3. One of the integration domains of J integral

For all these variants of calculations, the values of the stress intensity factor  $K_I$  are calculated, and the results are shown in Table 1. Numerical results for the stress intensity factor  $K_I$  are compared with the empirical value. The empirical value was obtained from the relation:

$$K_I^{emp} = \sigma F \left( \frac{a}{W}, \frac{L}{W} \right) \sqrt{\pi a} \quad (2)$$

and, based on the applied load and chosen value of the correction factor (Figure 3.11 in [2]), amounts

$$K_I^{emp} = 261.08 \text{ KPa} \sqrt{\text{mm}}. \quad (3)$$

For each obtained numerical value of stress intensity factor, there is a calculated error Er(%) given in Table 1. It was noticed that in case of coarse mesh the size of the integration domain should be considered, because it can happen that a small integration domain includes only a small number of nodes, and therefore get an error over 10%, so that result should be discarded as incorrect. In all other cases, the good agreement is obtained between numerical and empirical results. Increasing mesh density reduces the error and rapid convergence of the solution is apparent. Enrichment around crack tip with NT functions provides very good results even with coarse mesh. In all the cases when the NT enrichment was used, the error is below 3%. In cases with better mesh density can be noticed that the obtained numerical results are above the theoretical, leading to the conclusion that empirical solution read from the diagram given in the literature is not accurate enough.

Stress intensity factor  $K_I$  (10x10; 20x20; 40x40; 80x80) Table 1

| $\frac{r}{a}$ (%) | $K_I$ XFEM(H) 10x10 | Er (%) | $K_I$ XFEM(H+NT) 10x10 | Er (%) |
|-------------------|---------------------|--------|------------------------|--------|
| 10                | 121.15              | 53.59  | 137.88                 | 47.19  |
| 15                | 121.15              | 53.59  | 137.88                 | 47.19  |
| 20                | 121.15              | 53.59  | 170.28                 | 34.78  |
| 25                | 204.77              | 21.57  | 225.20                 | 13.74  |
| 30                | 241.27              | 7.59   | 255.73                 | 2.05   |
| 35                | 241.27              | 7.59   | 255.73                 | 2.05   |
| 40                | 241.27              | 7.59   | 257.78                 | 1.26   |
| 45                | 241.20              | 7.61   | 255.51                 | 2.13   |
| M.v.              | 191.66              | 26.59  | 212.00                 | 18.80  |

| $\frac{r}{a}$ (%) | $K_I$ XFEM(H) 20x20 | Er (%) | $K_I$ XFEM(H+NT) 20x20 | Er (%) |
|-------------------|---------------------|--------|------------------------|--------|
| 10                | 114.54              | 56.13  | 172.59                 | 33.89  |
| 15                | 254.15              | 2.65   | 262.27                 | 0.46   |
| 20                | 254.15              | 2.65   | 263.80                 | 1.04   |
| 25                | 253.90              | 2.75   | 261.74                 | 0.25   |
| 30                | 254.38              | 2.57   | 264.72                 | 1.39   |
| 35                | 252.60              | 3.25   | 260.36                 | 0.28   |
| 40                | 255.32              | 2.21   | 263.15                 | 0.79   |
| 45                | 253.93              | 2.74   | 261.45                 | 0.14   |
| M.v.              | 236.62              | 9.37   | 251.26                 | 3.76   |

| $\frac{r}{a}$ (%) | $K_I$ XFEM(H) 40x40 | Er (%) | $K_I$ XFEM(H+NT) 40x40 | Er (%) |
|-------------------|---------------------|--------|------------------------|--------|
| 10                | 257.51              | 1.37   | 266.41                 | 2.04   |
| 15                | 262.41              | 0.51   | 267.64                 | 2.51   |
| 20                | 262.18              | 0.42   | 266.46                 | 2.06   |
| 25                | 260.97              | 0.04   | 266.57                 | 2.10   |
| 30                | 260.84              | 0.09   | 265.53                 | 1.71   |
| 35                | 260.17              | 0.35   | 264.45                 | 1.29   |
| 40                | 260.43              | 0.25   | 264.35                 | 1.25   |
| 45                | 260.00              | 0.41   | 263.90                 | 1.08   |
| M.v.              | 260.56              | 0.20   | 265.66                 | 1.76   |

| $\frac{r}{a}$ (%) | $K_I$ XFEM(H) 80x80 | Er (%) | $K_I$ XFEM(H+NT) 80x80 | Er (%) |
|-------------------|---------------------|--------|------------------------|--------|
| 10                | 264.81              | 1.43   | 267.93                 | 2.62   |
| 15                | 265.06              | 1.52   | 267.49                 | 2.46   |
| 20                | 264.59              | 1.35   | 266.70                 | 2.15   |
| 25                | 263.90              | 1.08   | 266.32                 | 2.01   |
| 30                | 263.13              | 0.79   | 265.33                 | 1.63   |
| 35                | 262.91              | 0.70   | 264.98                 | 1.49   |
| 40                | 262.63              | 0.59   | 264.60                 | 1.35   |
| 45                | 262.28              | 0.46   | 264.23                 | 1.21   |
| M.v.              | 263.66              | 0.99   | 265.95                 | 1.86   |

After determining empirical values of the stress intensity factor, analytical solutions for stresses and displacements around the crack tip are calculated using the Table 2.

Analytical solutions for stresses and displacements Table 2

| Crack mode I  |  |
|---------------|--|
| $u_1$         | $\frac{K_I}{2\mu} \sqrt{r/(2\pi)} \cdot \cos \frac{\theta}{2} \left[ \kappa - 1 + 2 \sin^2 \frac{\theta}{2} \right]$ |
| $u_2$         | $\frac{K_I}{2\mu} \sqrt{r/(2\pi)} \cdot \sin \frac{\theta}{2} \left[ \kappa + 1 - 2 \cos^2 \frac{\theta}{2} \right]$ |
| $\sigma_{11}$ | $K_I / \sqrt{2\pi r} \cdot \cos \frac{\theta}{2} \left[ 1 - \sin \frac{\theta}{2} \sin \frac{3\theta}{2} \right]$    |
| $\sigma_{22}$ | $K_I / \sqrt{2\pi r} \cdot \cos \frac{\theta}{2} \left[ 1 + \sin \frac{\theta}{2} \sin \frac{3\theta}{2} \right]$    |
| $\sigma_{12}$ | $K_I / \sqrt{2\pi r} \cdot \sin \frac{\theta}{2} \cos \frac{\theta}{2} \cos \frac{3\theta}{2}$                       |

In the following analysis, numerically obtained stress values in the center of the element and analytically calculated values

for the same position were compared. Element, whose node was in the crack tip, was analyzed and obtained results are shown in Table 3 for different mesh densities and different enrichment functions around the crack tip.

The best matching results in case of enriching with NT functions are obtained with  $\sigma_{yy}$  component of stress, where the error in all variants of mesh density does not exceed 5%. Elements enriched with NT functions around the crack tip give a more accurate approximation of the stress field and a better agreement with the analytical results.

*Stress values in the center of the element (10x10; 20x20; 40x40; 80x80) Table 3*

| Stress                | Analytical result | XFEM(H) 10x10 | XFEM(H+NT) 10x10 |
|-----------------------|-------------------|---------------|------------------|
| $\sigma_x$ (error)    | 14.68             | 8.00 (45.5%)  | 8.82 (39.9%)     |
| $\sigma_y$ (error)    | 30.73             | 24.85 (19.1%) | 30.21 (1.7%)     |
| $\sigma_{xy}$ (error) | 3.33              | 3.36 (1.05%)  | 1.26 (62.1%)     |

| Stress                | Analytical result | XFEM(H) 20x20 | XFEM(H+NT) 20x20 |
|-----------------------|-------------------|---------------|------------------|
| $\sigma_x$ (error)    | 20.76             | 15.28 (26.4%) | 16.20 (22%)      |
| $\sigma_y$ (error)    | 43.46             | 37.61 (13.5%) | 44.33 (2%)       |
| $\sigma_{xy}$ (error) | 4.70              | 5.19 (10.4%)  | 2.01 (57.2%)     |

| Stress                | Analytical result | XFEM(H) 40x40 | XFEM(H+NT) 40x40 |
|-----------------------|-------------------|---------------|------------------|
| $\sigma_x$ (error)    | 29.36             | 25.79 (12.1%) | 26.82 (8.6%)     |
| $\sigma_y$ (error)    | 61.47             | 54.96 (10.6%) | 63.73 (3.7%)     |
| $\sigma_{xy}$ (error) | 6.65              | 7.62 (14.6%)  | 2.98 (55.2%)     |

| Stress                | Analytical result | XFEM(H) 80x80 | XFEM(H+NT) 80x80 |
|-----------------------|-------------------|---------------|------------------|
| $\sigma_x$ (error)    | 41.52             | 40.62 (2.2%)  | 41.79 (0.65%)    |
| $\sigma_y$ (error)    | 86.93             | 78.93 (9.2%)  | 90.75 (4.4%)     |
| $\sigma_{xy}$ (error) | 9.41              | 10.91 (15.9%) | 4.25 (54.8%)     |

In further analysis stress values according to the distance of the center of the element from the crack tip were compared. Figure 4 shows the comparative diagrams of normal stress  $\sigma_{yy}$  depending on the distance from the crack tip for different mesh densities, as well as a diagram of analytical solution. Based on the obtained results it can be concluded that the calculation results have a good agreement in the area around the crack tip for all sizes of mesh. All calculations show the character of the rapid growth of stress when asymptotically approaching the top of the crack. Because of the large impact of the distance from the crack tip to the center of the element to the value of the maximum stress, it is recommended to use a finer mesh around the crack tip.

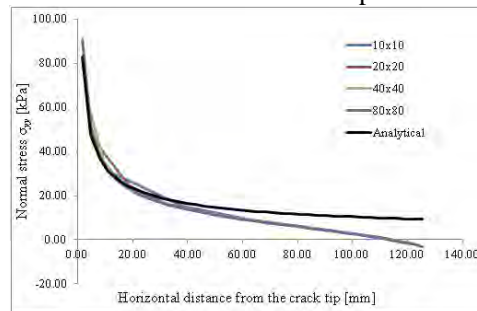


*Fig. 4. Normal stress  $\sigma_{yy}$  depending on the distance of the center of the element from the crack tip for different mesh densities*

Figure 5 shows the comparative diagrams of normal stress  $\sigma_{yy}$  depending on the distance of the center of the element

to the crack tip for the mesh density of 80x80 with enrichments H and H+NT. Based on the obtained results it can be concluded that the results for normal stresses are in agreement with the analytical result in both variants of enrichment. Stress values obtained enriching with NT functions give the expected slightly higher stresses, than the variant that uses only H functions.

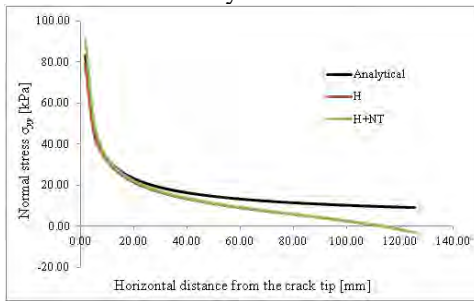


Fig. 5. Normal stress  $\sigma_{yy}$  depending on the distance of the center of the element to the crack tip for the mesh density of 80x80 with enrichments H and H+NT

Figure 6 shows comparative diagrams of the displacements of nodes in x direction depending on their vertical distance from a crack tip for mesh density 80x80, and also a diagram of the analytical solution obtained according to Table 2.

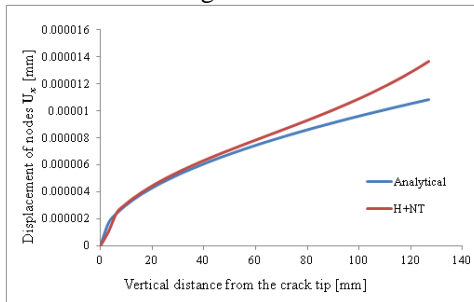


Fig. 6. Displacements of nodes in x direction depending on their vertical distance from a crack tip for mesh density 80x80

Figure 7 shows comparative diagrams of the displacements of nodes in y direction depending on their vertical distance from the crack tip for mesh density 80x80, as well as the diagram for the analytical solution according to Table 2.

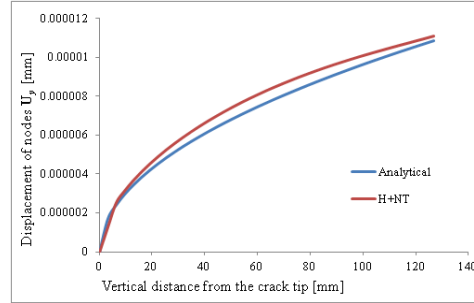


Fig. 7. Displacements of nodes in y direction depending on their vertical distance from the crack tip for mesh density 80x80

It can be concluded from the results that there is a good agreement between numerical and analytical results for the displacements of nodes in y direction depending on the vertical distance from the crack tip, as shown in Figures 6 and 7.

Impact of different enrichment around the crack tip for 10x10 mesh is shown in Figures 8 and 9.

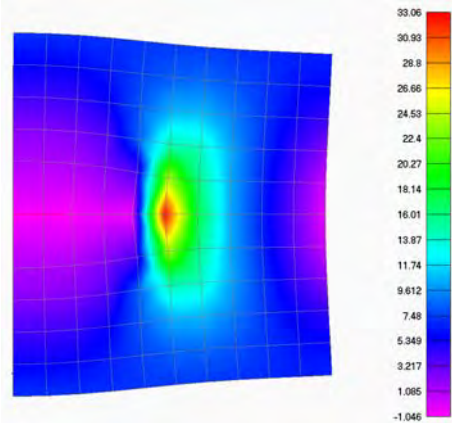


Fig. 8. Normal stress field  $\sigma_{yy}$  (XFEM(H)), 10x10

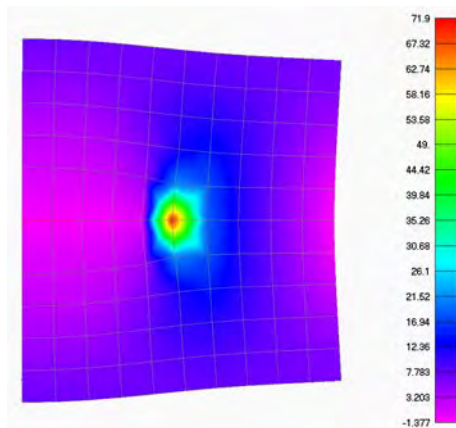


Fig. 9. Normal stress field  $\sigma_{yy}$   
(XFEM(H+NT)),  $10 \times 10$

It is obvious, in case of enrichment with NT, that there is rapid growth of stress when asymptotically approaching the crack tip, which is consistent with analytical solution.

#### 4. Conclusions

The accuracy of the XFEM method was analyzed in this paper. Analysis of the effect of mesh density and the types of enrichment in the XFEM on the accuracy of the numerical results is done by comparing them with empirical and analytical values.

From the obtained results, it can be concluded that the size of the integration domain should be considered because it can happen that a small integration domain includes only a small number of nodes. Increasing mesh density reduces the error and enrichment with NT functions give a more accurate approximation of the stress field and better agreement with the analytical results. It was seen that calculation results have a good agreement in the area around the crack tip for all sizes of mesh. All calculations show the character of the rapid growth of stress when asymptotically approaching top of

the crack. There is a good agreement between numerical and analytical results for the displacements of nodes in x and y directions depending on the vertical distance from the crack tip.

#### Acknowledgements

This research is supported with the Project TR32036 of Ministry of Education and Science, Republic of Serbia.

#### References

- [1] Belytschko, T., Black, T.: *Elastic crack growth in finite elements with minimal remeshing*, International Journal for Numerical Methods in Engineering, (1999) vol.45, no.5, p. 601-620.
- [2] Ćulafić, V.: *Introduction to Fracture Mechanics*, Faculty of Mechanical Engineering Podgorica, University of Montenegro, 1999.
- [3] Daux, C., Moes, N., Dolbow, J., Sukumur, N., Belytschko, T.: *Arbitrary cracks and holes with the extended finite element method*, International Journal for Numerical Methods in Engineering 48(12), 1741-1760, 2000.
- [4] Jovičić G., Živković M., Vulović S.: *Computational Fracture Mechanics and Fatigue*, Monograph, Faculty of Mechanical Engineering, 2011, ISBN 987-86-86663-65-8
- [5] Jovičić G., Živković M., Jovičić N.: *Numerical Simulation of Crack Modeling using Extended Finite Element Method*, Journal of Mechanical Engineering, Vol.55, No.9 pp. 549-554, UDC 620.178, ISSN 0039-2480, 2009.
- [6] Moes, N., Dolbow, J., Belytschko, T.: *A finite element method for crack growth without remeshing*, International Journal for Numerical Methods in Engineering, (1999), vol. 46, no. 1, p. 131-150.